ISRAEL JOURNAL OF TECHNOLOGY, Vol. 7, No. 6, 1969, pp. 469–475

Explosive Acceleration of Projectiles*

G. E. DUVALL**, J. O. ERKMAN*** AND C. M. ABLOW****
Stanford Research Institute, Menlo Park, California

Received June 23, 1969

ABSTRACT

The velocity of a small projectile accelerated by a plane layer of explosive is calculated for three cases: the explosive is bounded on both faces by voids and the projectile is either ahead of or behind the slab, and the explosive is bounded by void in front and a rigid wall behind with the projectile in front. The detonation gases are assumed polytropic with $\gamma = 3$ and the force on the projectile is given by a simple drag formula. The presence of the projectile is assumed not to affect the gas flow. The results show that it is relatively easy to accelerate the projectile to half the detonation velocity, but quite impractical to obtain, say, nine-tenths of detonation velocity. The first configuration mentioned above is most satisfactory for experimental purposes. The maximum stagnation pressure on the projectile is estimated to be the order of 150 kilobars, and this is assumed to represent the magnitude of the deformation stress leading to fragmention. The case of the projectile imbedded in the explosive surface is not considered.

NOTATION

x — space coordinate
t — time coordinate
D — detonation velocity
γ — polytropic exponent of detonation gases, $= 3.0$
c — sound velocity in detonation gases
l — Riemann velocity, $= 2c/(\gamma - 1)$
m — mass of projectile
s — position of projectile at time t
K — drag coefficient
A — cross-sectional area of projectile
ρ — density of detonation gases at (x, t)
u — particle velocity of detonation gases at (x, t)
1 — subscript denoting values at the Chapman-Jouguet plane
ρ_0 — initial explosive density
v — projectile velocity, ds/dt
a — explosive thickness
b — initial position of projectile
Q — acceleration parameter, $= 2\,K\rho_0 Aa/9m$
y — dimensionless space coordinate, $= s/a$
z — dimensionless time, $= Dt/a$
y' — dy/dz
y_∞' — terminal velocity of projectile
y_0, z_0 — initial values
d — explosive diameter
L — explosive length
σ_0 — deformation stress on projectile

I. INTRODUCTION

Problems of ballistic missile re-entry and space travel have caused attention to be focussed on the consequences of high velocity impact of small projectiles on various shield configurations (*Johnson*, 1969) and on methods for producing projectiles with suitably high velocities in the laboratory (*Lukasiewicz*, 1965). High explosives have sometimes been used for accelerating small projectiles in a configuration which consists of the projectile mounted on or near one face of a cylinder of explosive, which is detonated at the opposite face. The projectiles are then accelerated in the direction of travel of the detonation front. Variations of this configuration include encasing of the explosive in a

* Research sponsored in part by the Air Force Office of Scientific Research, Office of Aerospace Research, United States Air Force, under AFOSR grant No. AF AFOSR 1088–66.
** Now Professor of Physics, Washington State University, Pullman, Washington.
*** Now Physicist, Naval Ordnance Laboratory, Silver Spring, Md.
**** Senior Mathematician.

strong, heavy cylinder or forcing the detonation gases to flow through a nozzle and/or a blow-away barrel. Use of shaped charge jets is a different technique, but one which appears to yield higher velocities. It will not be discussed here.

In this paper we calculate the velocities of projectiles mounted at an arbitrary distance from the face of an explosive slab of finite thickness and of indefinite extent in transverse directions. These will provide upper limits to velocities produced by cylinders of finite diameter, encased or not, with projectiles mounted on an exposed face. The effect of a nozzle to direct the detonation gases adds another dimension to the problem and is not considered here.

The detonation is assumed to be a Chapman-Jouget detonation in which the detonation gases have a polytropic pressure-density relation with exponent γ, i.e.

$$p/p_1 = (\rho/\rho_1)^\gamma; \qquad l = 2c/(\gamma - 1)$$

$$u_1 = D/(\gamma + 1); \qquad c_1 = D\gamma/(\gamma + 1)$$

$$p_1 = \rho_0 D^2/(\gamma + 1); \quad \rho_1 = \rho_0(\gamma + 1)/\gamma.$$

We assume $\gamma = 3$, which assures that characteristics in the (x, t) plane are straight and simplifies the calculation. Experimental values of γ for condensed explosives are reasonably near this, ranging from 2.77 for 64/36 Comp. B to 3.17 for TNT (*Deal*, 1957). Computed values for the velocity of a rigid plate accelerated by explosive show that small variations of γ near three have little effect on the gas flow (*Aziz*, 1961). Consequently, we expect that values computed here are close to true upper limits to projectile velocities obtained in the geometry described.

The projectile to be accelerated is assumed to be initially at rest at an arbitrary distance from the explosive face, and it begins to move when the first detonation gases flow past it. Its presence produces a perturbation in the hydrodynamic field, but if the projectile is very small, the perturbation will be rapidly reduced to negligible magnitude by geometric divergence. The essential notion of the calculation is that the perturbation is negligible everywhere; the velocities thus calculated are correct for projectiles which are very small compared to explosive thickness.

The drag exerted on the projectile is assumed to be proportional to the square of the relative velocity, $(u - ds/dt)$, between projectile and gases and to the local gas density ρ. The equation of motion of the projectile is then

$$md^2s/dt^2 = \pm KA\rho(u - ds/dt)^2, \qquad (1)$$

where the sign is that of $u - ds/dt$, K is a drag coefficient and A is the projectile cross section presented to the gas flow. Initial conditions are $s = b$, $ds/dt = 0$ when the first signal from the detonation reaches the projectile. The procedure to be followed is to determine particle velocity, u, and density, ρ, for detonation gases at an arbitrary point (x, t) in the flow field. Then $u = u(s, t)$ and $\rho = \rho(s, t)$ along the trajectory. These are substituted into Eq. (1) and the resulting equation is integrated numerically.

II. GAS FLOW FIELD

Two explosive configurations are considered. In E1 the slab is bounded on either face by a void. In E2 the left boundary is rigid. In both cases the explosive faces are located at $x = 0$ and $x = a$ and the detonation is initiated at $x = 0$, $t = 0$.

A. *Case E1*

The flow field is represented in the (x, t) plane by Figure 1 and in the hodograph (u, l) plane by Figure 2.

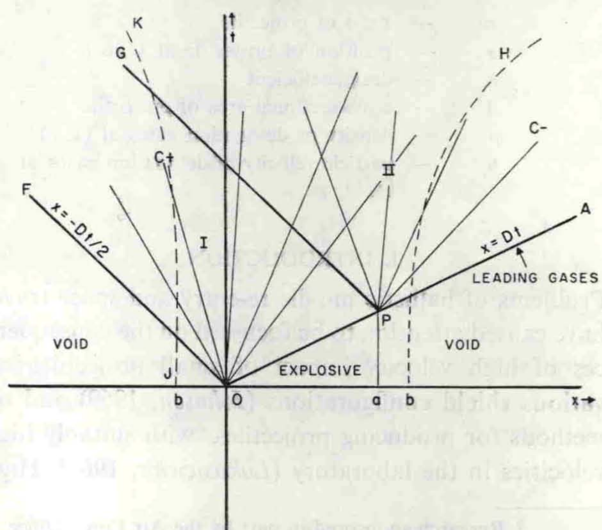

Figure 1

Flow field for unconfined explosive, case E1.

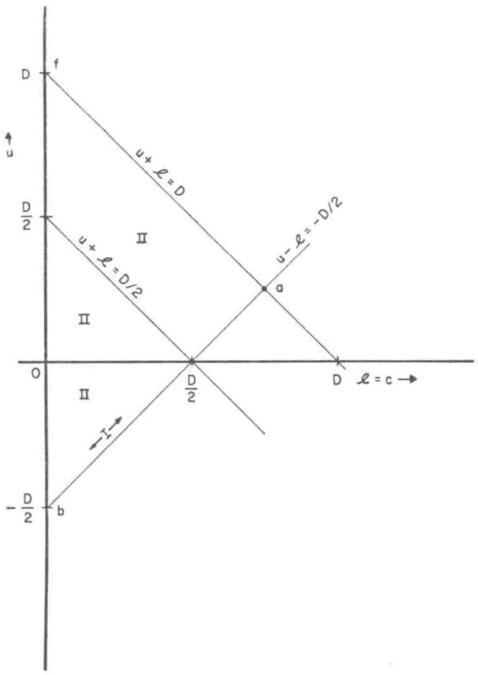

Figure 2
Hodograph plane for flow of Figure 1, case E1.

Region I in the (x, t) plane is bounded by the detonation front OP, by the C+ characteristic OF, and by the C− characteristic PG. The Chapman-Jouget state along OP is represented by point "a" in Figure 2, and the forward-facing rarefaction of Region I lies on the Γ- curve ab. Point b in Figure 2 is the image of OF in Figure 1, which consequently has a slope $dt/dx = -2/D$.

Reflection of the detonation wave from the free surface at $x = a$ (Figure 1) produces a rarefaction fan with straight C− characteristics centered at the point $P(x = a,\ t = a/D)$. The detonation gases are then accelerated into the void $(x > a)$ with limiting velocity D. Forward expansion is along af in Figure 2, and a region of overlap between the reflected rarefaction and the rarefaction following the detonation (the Taylor wave) is established as Region II of Figure 1.

For Region I:

$$\text{C+:} \quad u + c = x/t$$

$$\text{C−:} \quad u - c = -D/2$$

$$u = (x/t - D/2)/2 \tag{2a}$$

$$c = (x/t + D/2)/2 \tag{2b}$$

$$\rho = 8\rho_0(x/t + D/2)/9D \tag{2c}$$

Since Region I is a simple wave mapped on ab of Figure 2, any curve traversing Region I lies on ab. In particular the line PG, which separates Region II from Region I, lies on ab. PG is the leading C− characteristic of the fan passing through P of Figure 1, so

$$(dx/dt)_{PG} = u - c = (x - a)/(t - a/D)$$

But, since PG maps onto ab of Figure 2, $u - c = -D/2$ and

$$(x - a)/(t - a/D) = -D/2$$

PG is then parallel to OF, and for every other C− characteristic passing through P,

$$dx/dt = (x - a)/(t - a/D) > -D/2$$

For Region II:

$$\text{C−:} \quad u - c = (x - a)/(t - a/D)$$

$$\text{C+:} \quad u + c = x/t$$

$$u = [x/t + (x - a)/(t - a/D)]/2 \tag{3a}$$

$$c = [x/t - (x - a)/(t - a/D)]/2 \tag{3b}$$

$$\rho = 16\rho_0 c/9D \tag{3c}$$

Region II of Figure 1 maps into the triangle abf of Figure 2.

B. Case E2

The explosive is bounded at $x = 0$ by a rigid backing and at $x = a$ by a void. The flow field is shown in Figure 3. Region I behind the detonation front is a simple wave centered at (0, 0). Reflection at the free surface produces a backward-facing wave centered at A. The interaction of this wave with the Taylor wave and the rigid boundary produces the distinct and identifiable regions shown. Region III is a uniform state bounded by the last characteristic of the Taylor wave, OH, the leading characteristic of the reflection fan, AC, and the rigid boundary. The necessity for such a uniform region is shown in Figure 4. Here the point "a" is the Chapman-Jouget

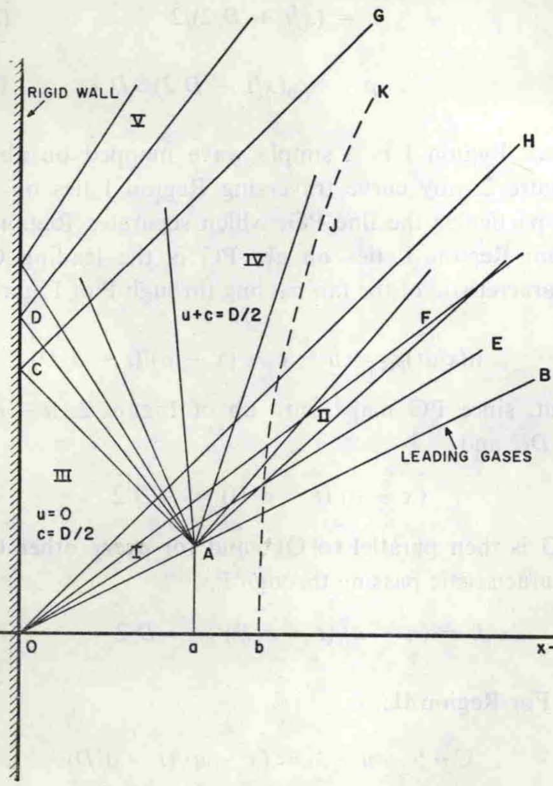

Figure 3
Flon field for confined explosive, case E2.

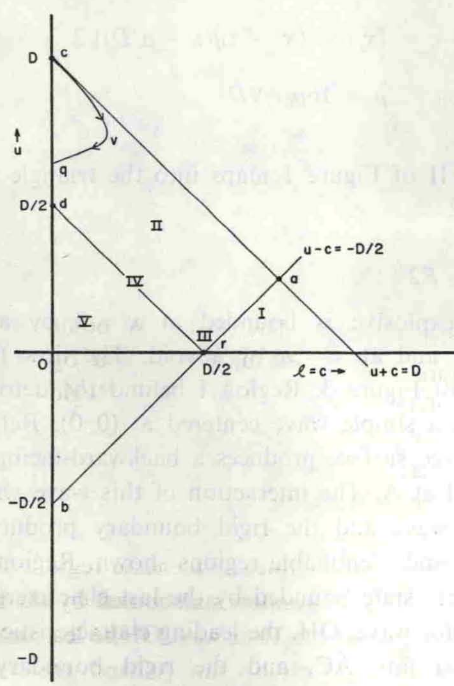

Figure 4
Hodograph mapping of flow field E1 of Figure 3.

state, and Region I lies along the Γ-characteristic ab. Region I terminates at $u = 0$, the condition imposed by the rigid boundary. Region III of Figure 3 is then mapped into the single point "III" of Figure 4. A traverse around the point A from OA to AB lies on or very close to the Γ+ characteristic ac in Figure 4. Region II of Figure 3 is mapped into the quadrilateral acdr of Figure 4. The boundary characteristic, OH, lies along dr. Region IV is again a simple wave region mapped onto the Γ+ characteristic $u + c = D/2$, shown in Figure 4. Region V is a mixed region resulting from interaction of the reflected rarefaction centered at A with its image in the $x = 0$ plane. The t-axis from C upward maps into the $u = 0$ axis, Or in Figure IV. The boundary CG corresponds to dr in Figure 4, and the open side of the triangular region V maps into Od of Figure 4. In symbols, these relations can be expressed as follows:

Region I: Same as Region I of Case E1.

Region II: Same as Region II of Case E1.

Region III:

$$u = 0 \tag{4a}$$

$$c = D/2 \tag{4b}$$

$$\rho = 8\rho_0/9 \tag{4c}$$

Region IV:

C+: $u + c = D/2$

C−: $u - c = (x - a)/(t - a/D)$

$$u = [D/2 + (x - a)/(t - a/D)]/2 \tag{5a}$$

$$c = [D/2 - (x - a)/(t - a/D)]/2 \tag{5b}$$

$$\rho = 16\rho_0 c/9D \tag{5c}$$

Region V:

C+: $u + c = (x + a)/(t - a/D)$

C−: $u - c = (x - a)/(t - a/D)$

$$u = x/(t - a/D) \tag{6a}$$

$$c = a/(t - a/D) \tag{6b}$$

$$\rho = 16\rho_0 a/9D(t - a/D) \tag{6c}$$

III. PROJECTILE MOTION

Three cases are considered: P1, the projectile is accelerated in the $+x$ direction for explosive configuration E1 with $b > a$; P2, the projectile is accelerated in the $-x$ direction for explosive configurattion E1 with $b < 0$; P3, the projectile is accelerated in the $+x$ direction for explosive configuration E2 with $b > a$. For $\gamma = 3$ Eq. (1) can be written

$$y'' = \pm\, 8Q(c/D)(u/D - y')^2 \tag{7}$$

where $y = s/a$, $z = Dt/a$, $Q = 2K\rho_0 Aa/9m$, and $y' \equiv dy/dz$. Initial conditions are $y = y_0$, $y' = 0$ at $z = z_0$. The three cases are distinguished by the expressions for u and c, given in the previous section.

A. Case P1, $b > a$

The projectile path is the dotted curve bH in Figure 1. Substituting Eqs. (3) into (7) with $x = s$ yields the equation to be solved for y:

$$y'' = Q[y/z - (y-1)/(z-1)] \\ [y/z + (y-1)/(z-1) - 2y']^2 \tag{8}$$

Motion of the projectile lies entirely within Region II since $u > 0$ for all $t > a/D$. Moreover the acceleration is never negative: $u > ds/dt$ initially and the difference diminishes as the projectile accelerates and the velocity of its local environment changes. When $u = ds/dt$, the projectile is in a region of constant particle velocity with no forces acting on it, so it will continue in that state indefinitely.

Eq. (8) has been integrated numerically for various values of $b/a > 0$ and for various Q. The results are shown in Figures 5 and 6 and in Table I. The terminal velocity is taken to be the last value obtained in the numerical integration, usually at $z > 10.0$. The effect of varying y_0 is illustrated in Table I. There is an appreciable increase of final velocity with y_0, the terminal velocity increasing as y_0 increases and the change being greater for small Q than for large. As y_0 approaches unity Eq. (7) becomes meaningless because it ignores the finite size of the object accelerated; it also becomes singular.

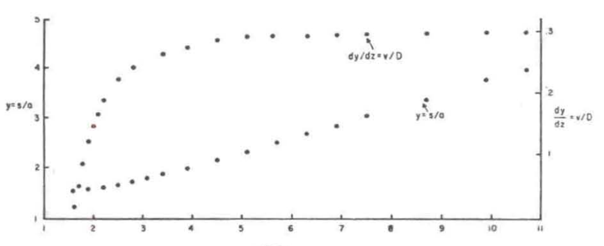

Figure 5

Trajectory and velocity of projectile for case P1; $b = 1.5a$, $Q = 1.0$.

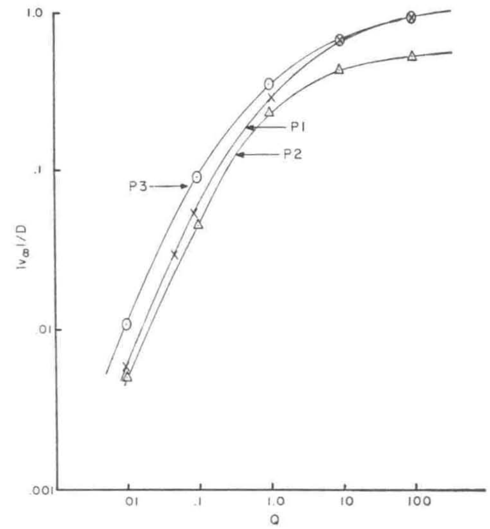

Figure 6

Terminal velocities of explosively accelerated projectiles. Initial positions: P1 and P3, $b/a = 1.1$; P2, $b/a = -.01$.

TABLE I

TERMINAL VELOCITIES OF EXPLOSIVELY ACCELERATED PROJECTILES $y_0 = x_0/a = -.01$ FOR P2. $v_\infty = D(dy/dz)_{z=\infty}$

	P1, P3	$\lvert v_\infty \rvert /D$			e		
Q	x_0/a	P1	P3	P2	P1	P2	P3
.01	1.1	.00587	.0109	.00503	1.09	.0015	1.06
	1.5	.00633					
.05	1.5	.0292					
.10	1.1	.0530	.0884	.0448	.989	.194	.766
	1.5	.0572					
1.0	1.01	.261					
	1.1	.284	.338	.220	.632	.408	.124
	1.5	.299	.351				
10.0	1.1	.632	.632	.408	.268	.808	.267
	1.5	.649					
100.0	1.1	.848	.848	.480	.103	1.50	.104
	1.5	.858					

Trajectories for all values of Q listed in Table I are similar to that shown in Figure 5, except that the final velocity is approached more rapidly for larger Q. In each case the trajectory is asymptotic to a straight line, $y = e + y_\infty' z$, where y_∞' is the asymptotic value of dy/dz. Terminal velocities for $y_0 = 0.0$ are plotted as curve P1 in Figure 6; values of e are given in Table I.

B. Case P2

The projectile path is the dotted curve JK of Figure 1. The equation of motion in Region I is obtained by substituting Eqs. (2) into Eq. (7). Defining y and z as before yields:

$$y'' = -Q(y/z + 1/2)(y/z - 1/2 - 2y')^2 \qquad (9)$$

Eq. (8) with a change of sign still applies in Region II. The projectile starts out in Region I and remains there so long as $(y - 1)/(z - 1) < -1/2$. When $(y - 1)/(z - 1) > -1/2$, Eq. (9) applies. When the projectile crosses the boundary between I and II, y and y' are continuous. Initial conditions are $y = b/a$, $y' = 0$ at $z = 2b/a$, $b < 0$. Terminal velocities are shown in Figure 6 and Table I.

C. Case P3

The projectile path is the dotted curve bJK of Figure 3. Eq. (8) is the equation of motion in Region II. In Region IV:

$$y'' = Q[1/2 - (y - 1)/(z - 1)] \qquad (10)$$
$$[1/2 + (y - 1)/(z - 1) - 2y']^2.$$

In Region V:

$$y'' = 8Q[y/(z - 1) - y']^2/(z - 1) \qquad (11)$$

Terminal velocities obtained from numerical integration are shown in Figure 6 and Table I. The transition from Region II to Region IV occurs when $y/z = 1/2$; that from IV to V when $(y + 1)/(z - 1) = 1/2$. When Q is large the projectile may not pass into Region IV at all, or may pass into it at such a late time that the event is no longer of interest or significance so far as its final velocity is concerned. It is this division of projectiles according to Q which produces the minimum in e for P3, Table I. For $Q \leqq 1.0$, the projectile passes into IV and V; for $Q \geqq 10$ it remains in II. This possibility can be inferred from Figure 4. Values of y and z can be transformed to (u, c) pairs and plotted to yield the curve cvq for $Q = 10$. Physically, this occurs because the particle first enters Region II where $u = D$ and $\rho = 0$, experiencing little acceleration. As time passes, ρ increases and u decreases but is still much larger than v. Then as time increases still more, ρ begins to decrease because the detonation gases have blown past the particle or are traveling backward. Moreover $u \to v$ so the acceleration is doubly-diminished. At the point q in Figure 4 the projectile has reached its terminal velocity, equal to the value of u at q. The form of this curve suggests that it would be useful for estimating y_∞'.

IV. DISCUSSION

General features of the results are shown in Figure 6. If one seeks maximum velocity, the projectile should be placed ahead of the explosive: cases P1 and P3. At lower velocities a rigid backing gives some additional impulse to the projectile, but, in each case calculated, is less effective than doubling the explosive thickness with no backing.

TABLE II

TERMINAL VELOCITY OF 200 MICRON SPHERE ACCELERATED BY EXPLOSIVE CYLINDER WITH $L/d = 3$; $d \equiv a$. $Q = a/30d$

a, cm	*Q*	*v/D*	*v m/sec*	*Explosive mass*
1	1.7	.35	3100	3.8 gm
10	17	.68	6000	8.5 lb
100	170	.89	7800	4.25 t

Detonation velocity = 8800 m/sec

The significance of the results can be better realized if we relate them to a particular experiment. Suppose a steel sphere of 200 microns diameter is to be accelarated by an explosive cylinder for which length/diameter equals three. Assume that the effective thickness of the equivalent slab is one diameter. Then the relation between explosive mass and terminal velocity is as shown in Table II. This shows clearly that terminal velocity increases so slowly with explosive mass that to achieve velocities much higher than about 6000 meters/second by direct explosive acceleration is quite impractical.

One anticipates that the rapid acceleration may subject the projectile to stresses which cause it to fracture or deform. These may be estimated by equating the stagnation pressure on the projectile to the maximum stress of deformation, σ_0. This yields

$$\sigma_0 = 2\rho_0 D^2 y''/9Q \qquad (12)$$

In the process of numerical integration, y'' was sometimes tabulated. The largest values of y''/Q recorded were $\sim .5$. Putting this into Eq. (12) with $\rho_0 = 1.7$ g/cc and $D = 8.8 \times 10^5$ cm/sec yields $\sigma_0 \sim 150$ kilobars. It is not surprising, then, that explosive-accelerated projectiles shatter. The remarkable thing is that sometimes they don't.

REFERENCES

AZIZ, A. K., H. HURWITZ AND H. M. STERNBERG, 1961. Energy transfer to a rigid piston under detonation loading, *Phys. Fluids.*, **4**, 380–384.

DEAL, W. E., 1957. Measurement of Chapman-Jouguet pressures of explosives, *J. Chem. Phys.*, **27**, 796.

JOHNSON, E. G., 1969. AIAA Hypervelocity Impact Conference, April 30–May 2, Cincinnati, Ohio. General Chairman, Elmer G. Johnson, Aerospace Research Laboratories, Wright Patterson AFB, Ohio. For information write to Meetings Dept., AIAA, 1290 Sixth Ave., New York, N.Y., 10019.

LUKASIEWICZ, J., 1965. Proc. of Fourth Hypervelocity Techniques Symposium, Arnold Engineering Development Center, Tullahoma, Tenn.

RINEHART, J. S. AND W. C. WHITE, 1952. Shapes of craters formed in plaster of Paris by ultraspeed pellets, *Am. J. Phys.*, **20**, 14.

SEIGEL, A. E., 1965. The theory of high speed guns, *AGARDOgraph* 91, North Atlantic Treaty Organization, Advisory Group for Aerospace Research and Development.